CYCLIC ARC PLASMA TESTS OF RSI MATERIALS USING A PREHEATER

D. A. Stewart

Ames Research Center
Moffett Field, California

ABSTRACT

This paper describes the results of a test program in which a preheater was used with an arc plasma stream to study the thermal response of samples of candidate reusable surface insulation (RSI) materials for space shuttle. The convective laminar heating environments simulated include both the shuttle Area 2 and 2P surface temperature and pressure histories as defined by NASA-MSC, while giving a uniform heating rate over the sample surface. A test cycle was composed of 35 minutes of radiant heating and 10 or 15 minutes of convective heating. The preheater was used to simulate the shuttle temperature history during the first and last portions of the test cycle, which could not be simulated by the air arc plasma flow. This investigation was conducted over a convective heating rate range from 225 to 450 kw/m^2 (20 to 40 Btu/ft^{2}sec) and at a surface pressure of approximately 810 N/m^2 (0.008 atm). The materials tested included LI-1542 (LMSC), HCF-MOD I and HCF-MOD III (MDAC), and REI-MOD I and REI-MOD 1A (GE). All materials had approximately a 240 kg/m^3 (15 lb/ft^3) density except the REI-MOD 1A, which had a 192 kg/m^3 (12 lb/ft^3) density. The LI-1542 is a high-purity silica rigidized fibrous material and the other materials are basically mullite fibrous materials rigidized with silica or mixed glass binders. The test samples were 10 cm (4 in) diameter cylinders. The cylinder thicknesses were 3.8 cm (1-1/4 in) and 4.8 cm (1-7/8 in). Test samples were mounted on a support consisting of a 0.15 cm (1/16 in) thick aluminum plate bonded to a fiberglass honeycomb and an aluminum baseplate 0.95 cm (3/8 in) thick. Thermocouples were installed within the RSI materials; the output of these and backplate temperature histories were recorded during each test cycle. Pre- and post-test data taken for each of the materials included magnified views, optical properties, and chemical analyses. The test results show that no catastrophic failure occurred during convective heating of the RSI materials tested; however, one of the coatings did fail, and this failure is discussed here. The test results also indicate that the HCF samples experience higher surface temperatures than the other materials at heating rates greater than $\dot{q}$ = 225 kw/m^2 (20 Btu/ft^{2}sec). The REI and LI-1542 coatings show noncatalytic wall behavior. Internal temperature response data for the materials are compared and are correlated with analytical predictions.

PROGRAM GOALS

(Figure 1)

This paper describes the results of a test program that uses an arc plasma stream to evaluate samples of reusable surface insulation (RSI) materials for space shuttle application. Arc plasma evaluations of these materials (silica and mullite) have been conducted by NASA and its contractors for approximately two years using stagnation-region and wedge-mounted samples with essentially an isothermal backwall (refs 1-4). In general, the procedure used in those tests was to insert the test sample directly into the arc plasma stream. In many cases, this resulted in the cracking of the mullite materials due to thermal stresses considerably in excess of those expected in the shuttle environment. A preheater was used in this study to more closely simulate the reentry temperature environment on the shuttle, thereby reducing the thermal stresses to more realistic values.

The primary program goals were to evaluate changes in morphology, optical properties, and chemical composition of the RSI coatings after cyclic arc plasma exposure. The secondary program goals were to evaluate thermal response and surface temperature of the RSI materials during arc plasma exposures. The RSI materials were tested using nearly adiabatic backface model configurations. The investigation was conducted in two parts using second and third generation RSI materials supplied through the Manned Spacecraft Center, RSI contracts, and in-house programs by General Electric, Lockheed, and McDonnell Douglas. The first part of the investigation dealing with coating morphology changes, thermal response, surface temperature, and variation of optical properties of the coatings are discussed in this paper. The second part of the investigation dealing with coating morphology and chemistry changes is reported in another paper in this volume entitled, "Chemical and Morphological Change of Reusable Surface Insulation Coatings as a Function of Convectively Heated Cyclic Testing," by D.B. Leiser, D.A. Stewart, and H.E. Goldstein.

PROGRAM GOALS

EVALUATE:

- CHANGES OF COATING MORPHOLOGY AND CHEMISTRY
- THERMAL RESPONSE OF RSI TILES
- SURFACE TEMPERATURE - CATALYTIC WALL ACTIVITY
- OPTICAL PROPERTIES

Figure 1

MODEL CONFIGURATION

(Figure 2)

The model configurations shown in figures 2 and 3 are 10 cm (4 in) diameter by 3.8 cm (1-1/2 in) thick disks made from RSI materials. The disks are mounted to a 0.15 cm (1/16 in) thick aluminum plate. An adiabatic backwall condition was approximated by using a 1.3 cm (1/2 in) thick fiberglass honeycomb material as insulation between the aluminum backplate and the mounting plate. The first model configuration is shown in figure 2. This configuration consisted of a single RSI sample secured to the backplate with 0.013 cm (.005 in.)thick RTV adhesive.

Chromel-alumel thermocouples were installed through the center of the RSI material at depths of 0.31, 0.64, 1.3, and 3.2 cm (1/8, 1/4, 1/2, and 1-1/4 in.)from the coated surface. Two additional thermocouples were installed at the center and at 3.8 cm (1-1/2 in.)from the center in the 0.15 cm (1/16 in) aluminum backplate. Surface morphology changes, thermal response, and surface temperature data were obtained using this model configuration.

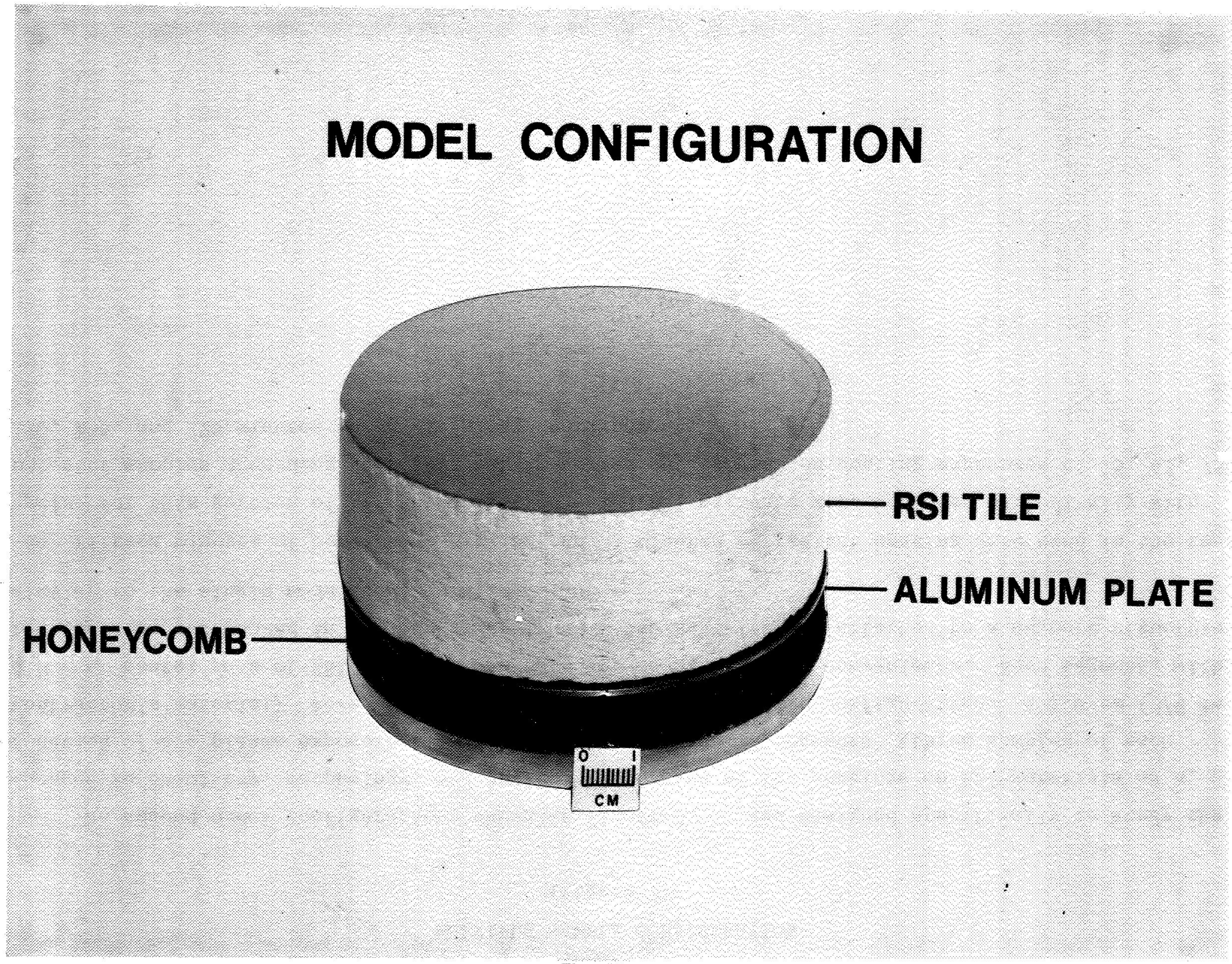
MODEL CONFIGURATION
RSI TILE
ALUMINUM PLATE
HONEYCOMB
0 1
CM

Figure 2

MULTIPLE SAMPLE CONFIGURATION

(Figure 3)

The second model configuration, shown in figure 3, was designed specifically to study the changes in chemistry, morphology, and optical properties of the coatings on RSI materials as a function of arc plasma exposure time. Nine 40° wedge-shaped segments (three samples of each contractor's material) were used to make up the multiple-sample configuration. A 1.0 cm (3/8 in.) diameter center post of RSI material was used for model assembly convenience. Each segment, with two brass screws bonded in the backside with RTV 560 adhesive, is attached to a support structure similar to the single model configuration.

Fifteen minutes of convective heating and 35 minutes of radiant heating were used in the test cycles for this portion of the investigation. The RSI segments were replaced periodically with untested samples according to a text matrix worked out to provide coating exposures of 15, 45, 75, 120, 135, and 225 minutes to an arc plasma environment.

MULTIPLE SAMPLE CONFIGURATION

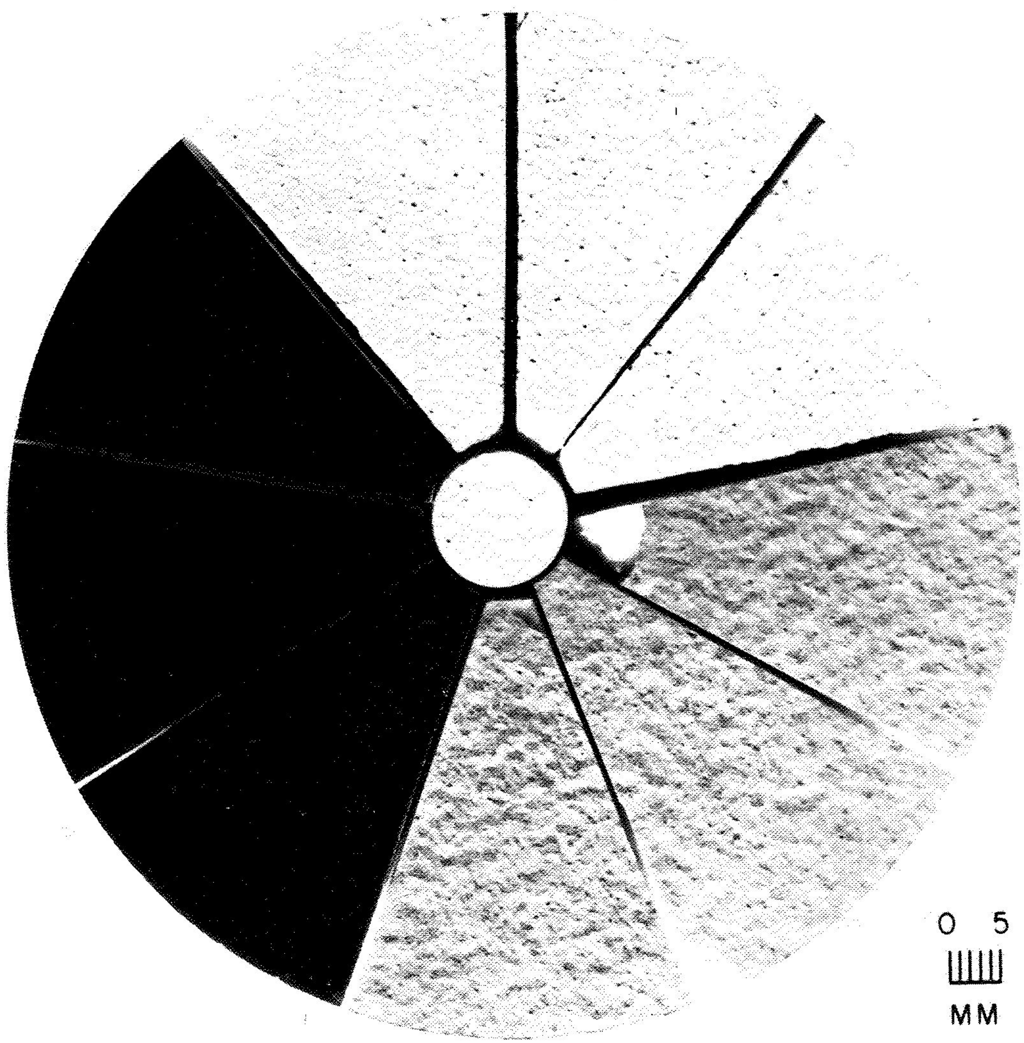

Figure 3

TRAJECTORY SIMULATION USING ARC PLASMA FACILITY AND PREHEATER

(Figure 4)

The model configuration was mounted in the center of a 20 cm (8.0 in) diameter flat-face water cooled copper cylindrical sample holder. The sample holder also contained a calorimeter and two 0.1 cm (0.040 in) diameter pressure orifices located 90° apart and circumferentially on a radius of 6.3 cm (2-1/2 in). A radiant preheater, consisting of a Kanthal-1A wire coil positioned in a spherical cavity in the base of a 60° blunted cone, is shown in front of the sample holder. The blunted cone was made from high purity silica, coated with an emittance agent of silica bonded chromium oxide, and attached to a water-cooled movable support.

Comparisons of the shuttle temperature and pressure reentry simulations with the NASA Area 2P trajectory are shown to the right of this figure. The preheater was used for the initial and final portions of the simulation, and an arc plasma stream was used for the high temperature portion (600 to 1200 seconds) of the simulation. The preheater heated the sample surface to 1367°K (2000°F) at which time the preheater and sample holder were both translated into the arc plasma flow exiting from a 61 cm (24 in) diameter nozzle. The preheater was then removed from the arc plasma stream and the sample was exposed to the arc plasma flow. The reverse procedure was used with the preheater during the cool-down portion of the simulation. During the cool-down (1200 to 3000 seconds) portion of the surface temperature simulation, the arc plasma stream was turned off and the test chamber pressure was increased to simulate the surface pressure history during the later phase of reentry.

Sample surface environmental conditions were determined using measurements from an impact-pressure probe and a 3.2 cm (1-1/4 in) diameter hemispherical calorimeter probe located on the swing-in arm and assuming an equilibrium boundary-layer edge condition. In addition, the stagnation point heating rate to the sample was obtained by correcting the calorimeter measurement taken from the sample holder and using the convective heating rate distribution theory of Lees (refs. 5-6). A more detailed description of the facility is given in reference 7.

TRAJECTORY SIMULATION USING ARC PLASMA FACILITY AND PREHEATER

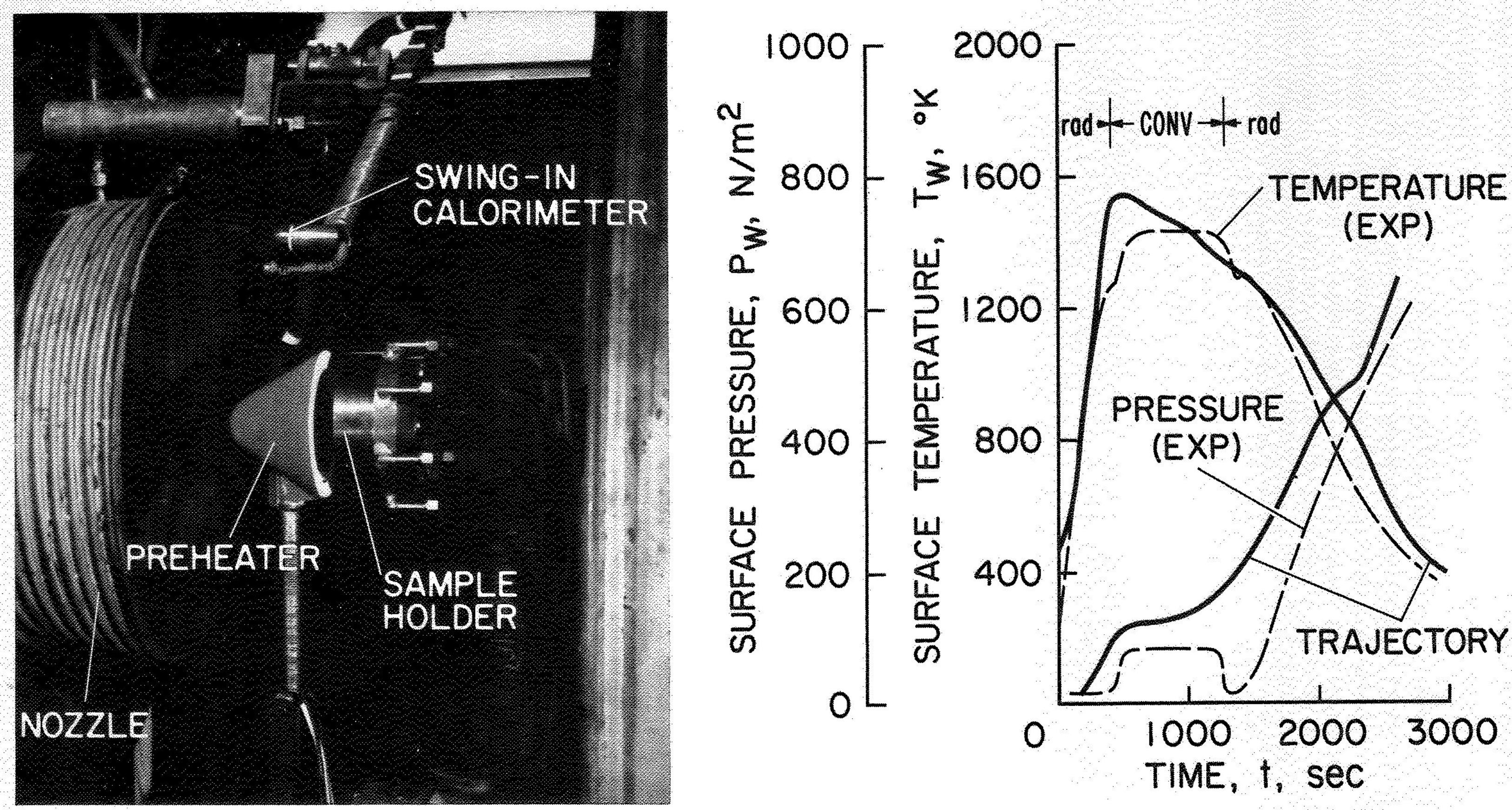

Figure 4

SUMMARY OF ARC PLASMA/RADIANT HEATED TEST RESULTS ON RSI CANDIDATE MATERIALS

$D = 10$ cm, $P_s = 810$ N/m^2

(Figure 5)

This figure summarizes the tests performed on the RSI candidate materials using the single 10 cm (4.0 in) diameter model configuration. The total number of test cycles for each material given is for more than one RSI sample of LI-1542, HCF-MOD III, and REI-MOD 1A. One hundred and seventy test cycles, consisting of 35 minutes of radiant heating and 10 minutes of convective heating were conducted on these materials. Each RSI material was exposed to test conditions of cold-wall stagnation point heating rates ($\dot{q}$) from 225 kw/m^2 (20 Btu/ft^{2}sec) to 450 kw/m^2 (40 Btu/ft^{2}sec) with a surface pressure (P_s) of approximately 810 N/m^2 (0.008 atm). The surface temperature (Tw) varied from 1311°K (1900°F) to 1627°K (2469°F) on these RSI coatings. The largest variation of the surface temperature 1367°K (2000°F) to 1627°K (2469°F) was observed on the HCF-MOD III coatings. The smallest variation in surface temperature, 1367°K (2000°F) to 1478°K (2200°F), was observed on the LI-1542 coatings. The backplate temperatures (T_{BP}) for the various RSI materials tested are included in the figure. Although these measurements are not directly applicable to the shuttle, they do illustrate the difference in thermal conductivity of the various RSI materials tested.

Two LI-1542 samples were tested. The first sample was tested for 20 cycles at heating rates from $\dot{q}$ = 225 kw/m^2 (20 Btu/ft^{2}sec) to $\dot{q}$ = 340 kw/m^2 (30 Btu/ft^{2}sec). The coating on this sample became contaminated during the 20th test cycle due to the failure of a waterline on the model support system. The surface temperature data from these tests at $\dot{q}$ = 225 kw/m^2 (20 Btu/ft^{2}sec) are used in the catalytic wall activity results. A second LI-1542 sample was then tested for 22 cycles at heating rates from $\dot{q}$ = 340 kw/m^2 (30 Btu/ft^{2}sec) to $\dot{q}$ = 450 kw/m^2 (40 Btu/ft^{2}sec).

Three HCF samples were tested. The first was an HCF-MOD I and the other two were HCF-MOD III samples. The HCF-MOD I sample was tested for 30 cycles at heating rates from $\dot{q}$ = 225 kw/m^2 (20 Btu/ft^2 sec) to $\dot{q}$ = 450 kw/m^2 (40 Btu/ft^{2}sec). Repeat cycles at heating rates of $\dot{q}$ = 340 kw/m^2 (30 Btu/ft^{2}sec) and $\dot{q}$ = 225 kw/m^2 (20 Btu/ft^{2}sec) were also conducted to check for possible changes in catalytic activity of the coating. The second HCF sample, made from HCF-MOD III material was tested for 28 cycles at heating rates from $\dot{q}$ = 225 kw/m^2 (20 Btu/ft^{2}sec) to $\dot{q}$ = 450 kw/m^2 (40 Btu/ft^{2}sec). The third HCF sample tested, also made from HCF-MOD III material, had in-depth thermocouples installed at a radius of 3.8 cm (1-1/2 in) and through the center of the sample (R = 0). This sample was tested at heating rates from $\dot{q}$ = 260 kw/m^2 (23 Btu/ft^{2}sec) to $\dot{q}$ = 450 kw/m^2 (40 Btu/ft^{2}sec) to determine the relative change in thermal response through a mullite tile as a function of radial position and heating rate.

Four REI samples were tested. First, an REI-MOD I material was tested 33 cycles at heating rates from $\dot{q}$ = 225 kw/m^2 (20 Btu/ft^{2}sec) to $\dot{q}$ = 450 kw/m^2 (40 Btu/ft^{2}sec). Next, three samples made from REI-MOD 1A material having a density of 192 kg/m^3 (12 lb/ft^3) were tested. The first of these samples, identified with an asterisk, had a thickness of 4.8 cm (1-7/8 in.). This REI-MOD 1A sample was tested at $\dot{q}$ = 340 kw/m^2 (30 Btu/ft^{2}sec) to provide temperature distribution data for comparison with the other REI materials on an equivalent section weight basis. The second of these REI samples, having a thickness of 3.8 cm (1-1/2 in.),was tested at $\dot{q}$ = 275 kw/m^2 (24 Btu/ft^{2}sec). After severe cracking near the edge of the coating occurred on both of these REI-MOD 1A samples, a third sample,which had a 7.6 cm (3.0 in) diameter,was tested. This latter REI-MOD 1A sample was tested for 22 cycles at heating rates from $\dot{q}$ = 340 kw/m^2 (30 Btu/ft^{2}sec) to $\dot{q}$ = 450 kw/m^2 (40 Btu/ft^{2}sec).

Figures 6 through 9 show the general morphology characteristics of representative LI-1542, HCF-MOD III, and REI-MOD 1A materials after various arc plasma cyclic exposures.

SUMMARY OF ARC PLASMA/RADIANT HEATED TEST RESULTS ON RSI CANDIDATE MATERIALS

$D = 10$ cm, $P_s = 810$ N/m^2

MATERIAL	SAMPLE NUMBER	TOTAL TEST CYCLES	$\dot{q}$ kw/m^2	H_{eo} MJ/kg	T_W °K	T_{BP} °K	REMARKS
LI-1542	1	20	225-340	8.3-11.0	1367-1430	333-335	CONTAMINATED
	2	22	225-450	8.3-13.8	1367-1478	333-341	NO CRACKS
HCF-MOD I	1	32	225-450	8.5-13.6	1311-1575	374-421	NO CRACKS
MOD III	2	28	225-450	8.8-14.8	1367-1627	372-422	CRACK-RAISED AREA
MOD III	3	4	260-450	10.0-13.3	1483-1622	387-410	NO CRACK
REI-MOD I	1	33	225-450	8.4-13.8	1381-1509	377-406	SMALL EDGE CRACK
*MOD IA	2	3	340	11.0	1456	344	SEVERE CRACKS
MOD IA	3	6	275	9.4	1413	377	SEVERE CRACKS
MOD IA	4	22	225-450	8.4-13.2	1381-1502	377-434	NO CRACKS

*4.8 CENTIMETER THICK SAMPLE

Figure 5

LI-1542 TEST SAMPLE

(Figure 6)

A front surface view of the LI-1542 sample after 22 cycles is shown in the center of this figure. This sample was tested for ten cycles at $\dot{q}$ = 340 kw/m^2 (30 Btu/ft^{2}sec), ten cycles at $\dot{q}$ = 450 kw/m^2 (40 Btu/ft^{2}sec), a repeat cycle at $\dot{q}$ = 340 kw/m^2 (30 Btu/ft^{2}sec), and one cycle at $\dot{q}$ = 225 kw/m^2 (20 Btu/ft^{2}sec). Pre- and post-test magnified views of a 0.30 cm (1/8 in) diameter area at the center and near the edge of the coating were taken at a magnification of 27X with a Macro-Dia apparatus. Some variation in the appearance of the magnified views are apparently due to slightly different angles of the incident light used to illuminate the surface of the sample. A pre-test magnified view of the coating is shown in the upper left corner of the figure. A magnified view near the edge of the coating after ten cycles at a heating rate of $\dot{q}$ = 340 kw/m^2 (30 Btu/ft^{2}sec) is shown in the upper right corner. Post-test magnified views are shown in the bottom half of the figure. The left view was taken at the center and the right view was taken near the edge of the sample. The figure shows the morphology changes of the LI-1542 coating are minimal after 22 test cycles at heating rates from $\dot{q}$ = 225 kw/m^2 (20 Btu/ft^{2}sec) to $\dot{q}$ = 450 kw/m^2 (40 Btu/ft^{2}sec).

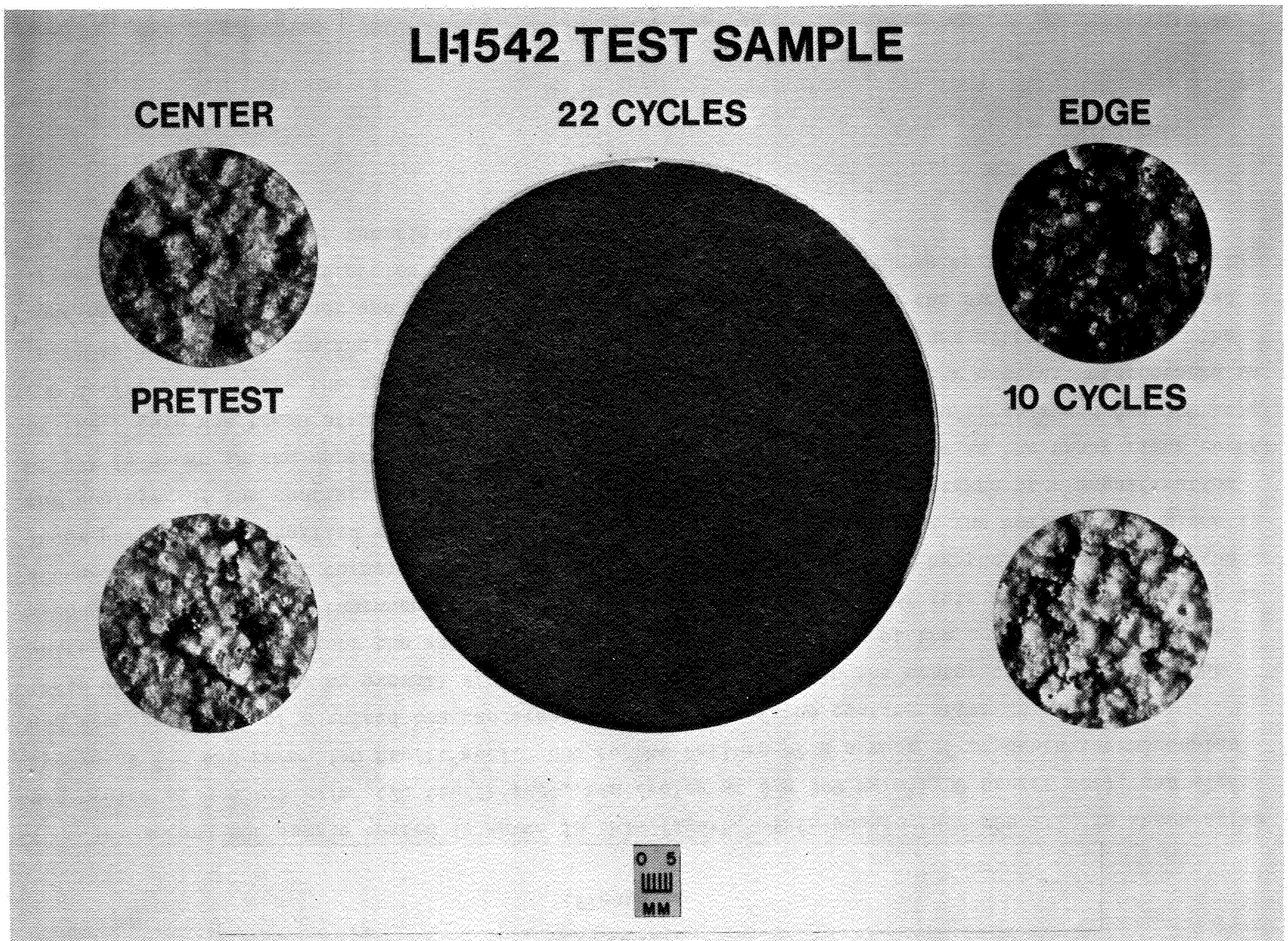
LI-1542 TEST SAMPLE
CENTER
22 CYCLES
EDGE
PRETEST
10 CYCLES
0 5
MM

Figure 6

HCF-MOD III
(Figure 7)

The second HCF sample tested is shown in this figure. This sample, HCF-MOD III, is shown after ten cycles at $\dot{q}$ = 225 kw/m^2 (20 Btu/ft^{2}sec), ten cycles at $\dot{q}$ = 340 kw/m^2 (30 Btu/ft^{2}sec), and eight cycles at $\dot{q}$ = 450 kw/m^2 (40 Btu/ft^{2}sec). Due to the failure of a number of in-depth thermocouples and the appearance of a raised cracked area at the center of the coating after 28 cycles the tests were terminated. An overall view of the coating is shown in the center of the figure. The white area at the center of the sample surface is the raised portion of the coating caused by the mechanical failure of a thermocouple just under it. A magnified view of this area of the coating is shown in the lower left corner of the figure. Note the crack (indicated by the shaded area in the lower part of the magnified view) and the advanced state of the foaming of the borosilicate glass in the sublayer of the coating. Again, a pre-test photograph of the coating taken at a magnification of 27X is shown in the upper left corner of the figure. The magnified view in the upper right corner of the figure was taken after ten test cycles each at $\dot{q}$ = 225 kw/m^2 (20 Btu/ft^{2}sec) and $\dot{q}$ = 340 kw/m^2 (30 Btu/ft^{2}sec). Note the apparent removal of the potassium silicate sealer coating, microcracks in the remainder of the coating, and forming of the sublayer borosilicate glass after 20 cycles. The coating has become rougher and the foaming of the borosilicate glass in the sublayer has increased after an additional eight cycles at $\dot{q}$ = 450 kw/m^2 (40 Btu/ft^{2}sec), as shown by the magnified view in the lower right corner of the figure.

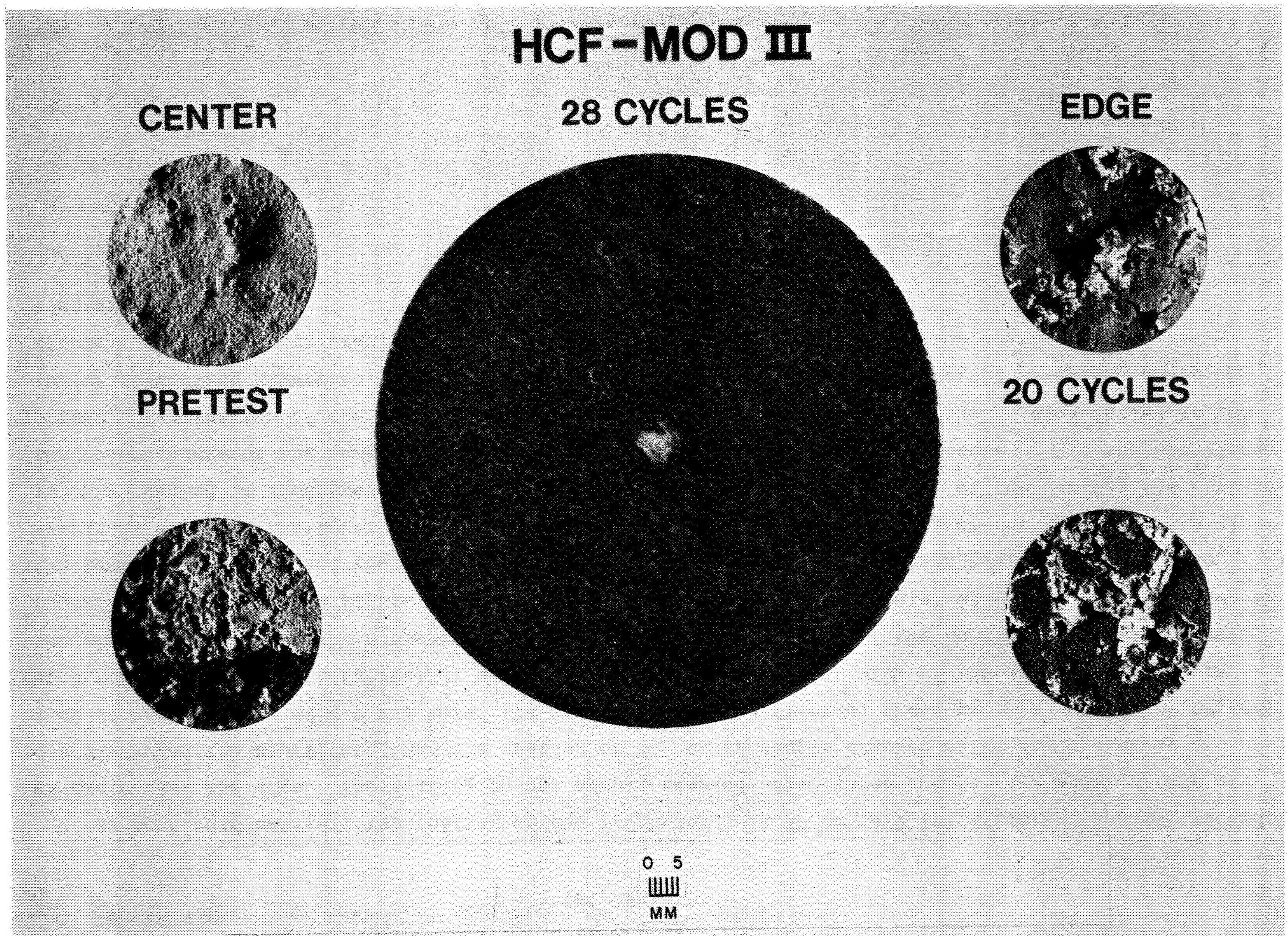

Figure 7

REI-MOD 1A
(Figure 8)

As mentioned earlier, the coating on the two REI-MOD 1A 10 cm (4.0 in) diameter samples cracked severely near the edge. The coating on one sample cracked after three cycles at a heating rate of $\dot{q}$ = 340 kw/m^2 (30 Btu/ft^2sec) and the coating on the other sample cracked after six cycles at a reduced heating rate of $\dot{q}$ = 275 kw/m^2 (24 Btu/ft^2sec). The first of these samples, which was tested at $\dot{q}$ = 340 kw/m^2 (30 Btu/ft^2sec), is shown in this figure. A front view of the sample is shown in the center of the figure. A pre-test magnified view of the center of the coating is shown in the upper left corner of the figure. A post-test magnified view of the center of the coating is shown in the lower left corner and the RSI substrate material just under the coating near the edge of the sample is shown in the lower right corner of the figure. Apparent foaming of the low viscosity glass in this coating is indicated by the post-test magnified view of the center of the coating and explains the color change of the coating from a brownish-green to a gray after exposure to the arc plasma stream. Examination of the coating pieces after the tests indicated that the coating failed at the substrate coating interface. The coating failure is attributed to high thermal stresses caused by either high temperature gradients or a large change in the thermal expansion coefficient of the coating material.

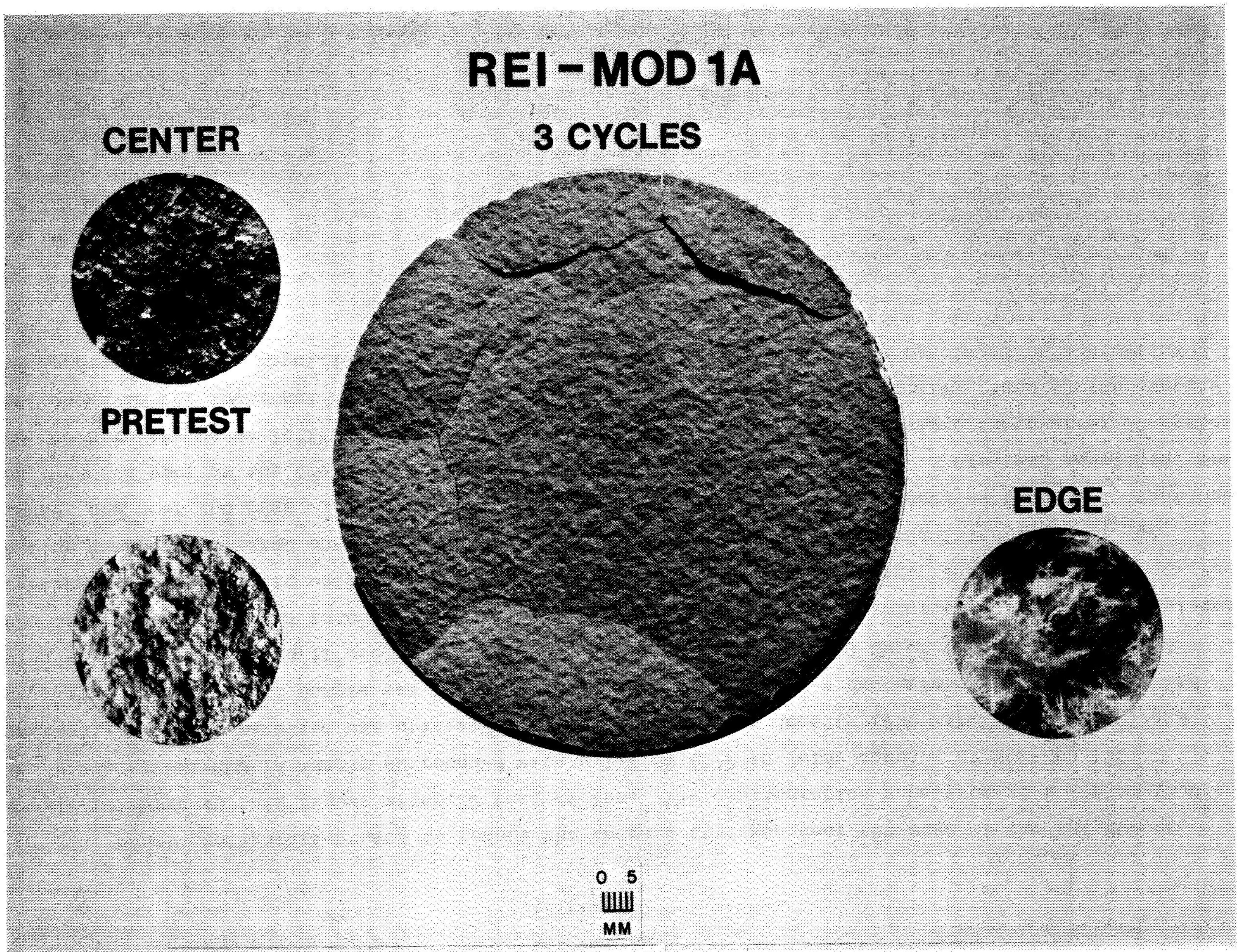

Figure 8

REI-MOD 1A

(Figure 9)

The model configuration used to reduce the thermal stresses near the edge of the REI-MOD 1A sample is shown in this figure after 22 test cycles. The configuration consisted of a 7.6 cm (3.0 in.)diameter REI-MOD 1A sample surrounded with a 1.2 cm (1/2 in.)wide annulus of HCF-MOD III material. The HCF material was utilized because of its higher density (240 kg/m^3, 15 lb/ft^3) and availability. This REI sample was tested for ten cycles each at $\dot{q}$ = 340 kw/m^2 (30 Btu/ft^2sec) and at $\dot{q}$ = 450 kw/m^2 (40 Btu/ft^2sec). A repeat cycle was taken at $\dot{q}$ = 340 kw/m^2 (30 Btu/ft^2sec), and one additional cycle was taken at $\dot{q}$ = 225 kw/m^2 (20 Btu/ft^2sec) to determine the effect of arc plasma testing on the catalytic wall activity and total emissivity of the coating. The coating did not crack during these tests based on visual observations. Pre-test and post-test magnified views of the center and near the edge of the coating are shown in the figure. These views, as previously mentioned, represent a spot on the coating surface having a 0.3 cm (1/8 in) diameter. A pre-test magnified view is shown in the upper left corner of the figure. Two post-test magnified views taken after 22 cycles are shown in the lower half of the figure. Again, foaming of the low viscosity glass in the coating is apparent from the magnified views and explains the color change of the coating from a brownish-green to a gray.

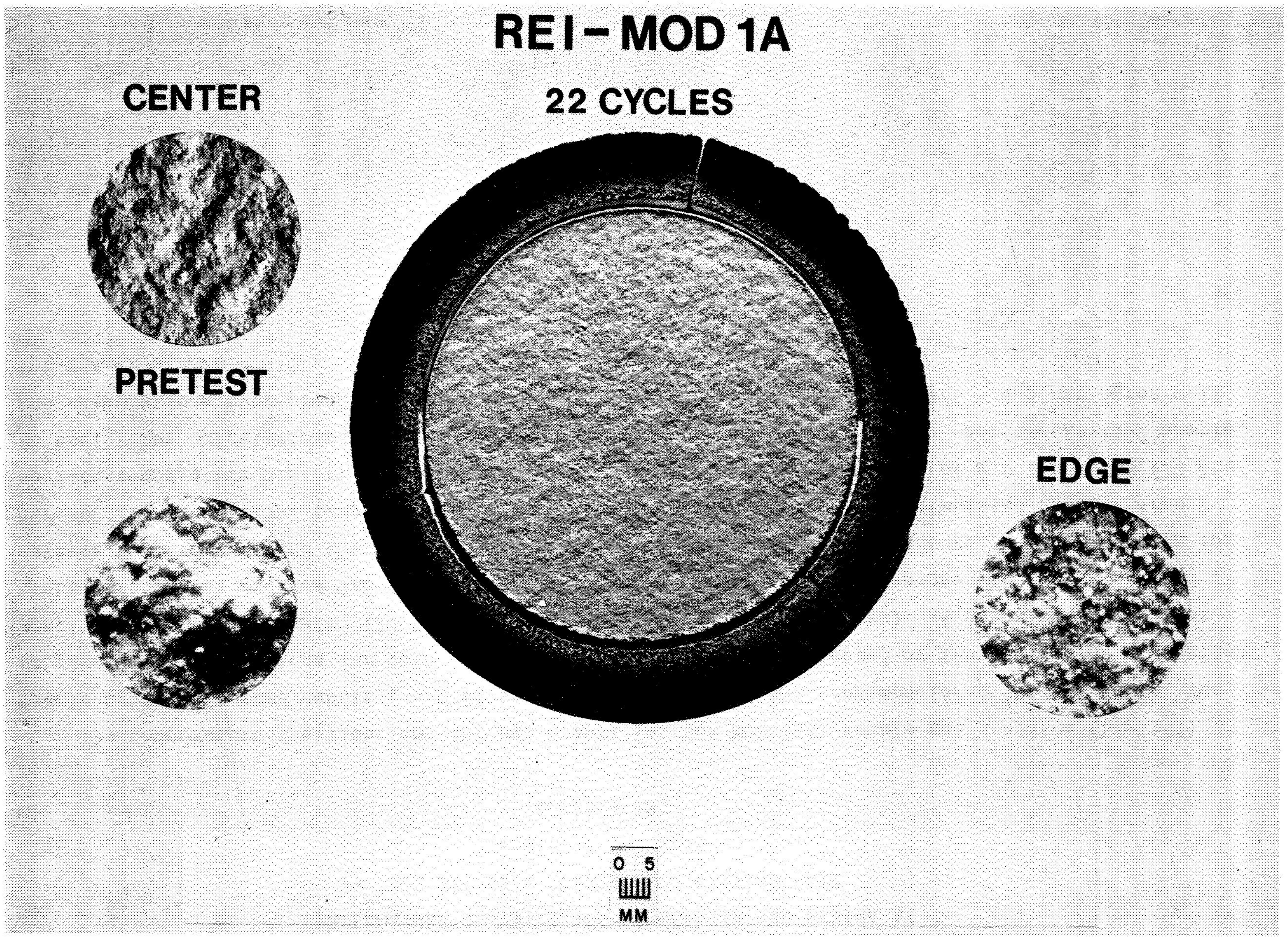

Figure 9

TEMPERATURE DISTRIBUTION OF MULLITE AND SILICA AT

1200 SEC AS A FUNCTION OF HEATING RATE

Density = 240 kg/m^3

(Figure 10)

The temperature distributions through a mullite (HCF-MOD III) sample and a silica (LI-1542) sample having the same density, are plotted as a function of the nondimensional RSI thickness. The temperature distributions for both materials were relatively unaffected by increasing the stagnation heating rate from 225 kw/m^2 (20 Btu/ft^2sec) to 450 kw/m^2 (40 Btu/ft^2sec). A one dimensional heat transfer computer program was used to calculate the in-depth thermal response using the measured surface temperatures and thermal conductivity data supplied by the contractors. The prediction for HCF-MOD III and LI-1542 temperature distributions at 1200 seconds into a simulated shuttle Area 2 surface temperature history are compared with experiment at a heating rate of $\dot{q}$ = 225 kw/m^2 (20 Btu/ft^2sec). The calculations agree reasonably well with the HCF-MOD III data. For the LI-1542 sample, the calculations over-predict the in-depth temperature data for values of $X/L < 0.5$ and agree well for values of $X/L > 0.5$.

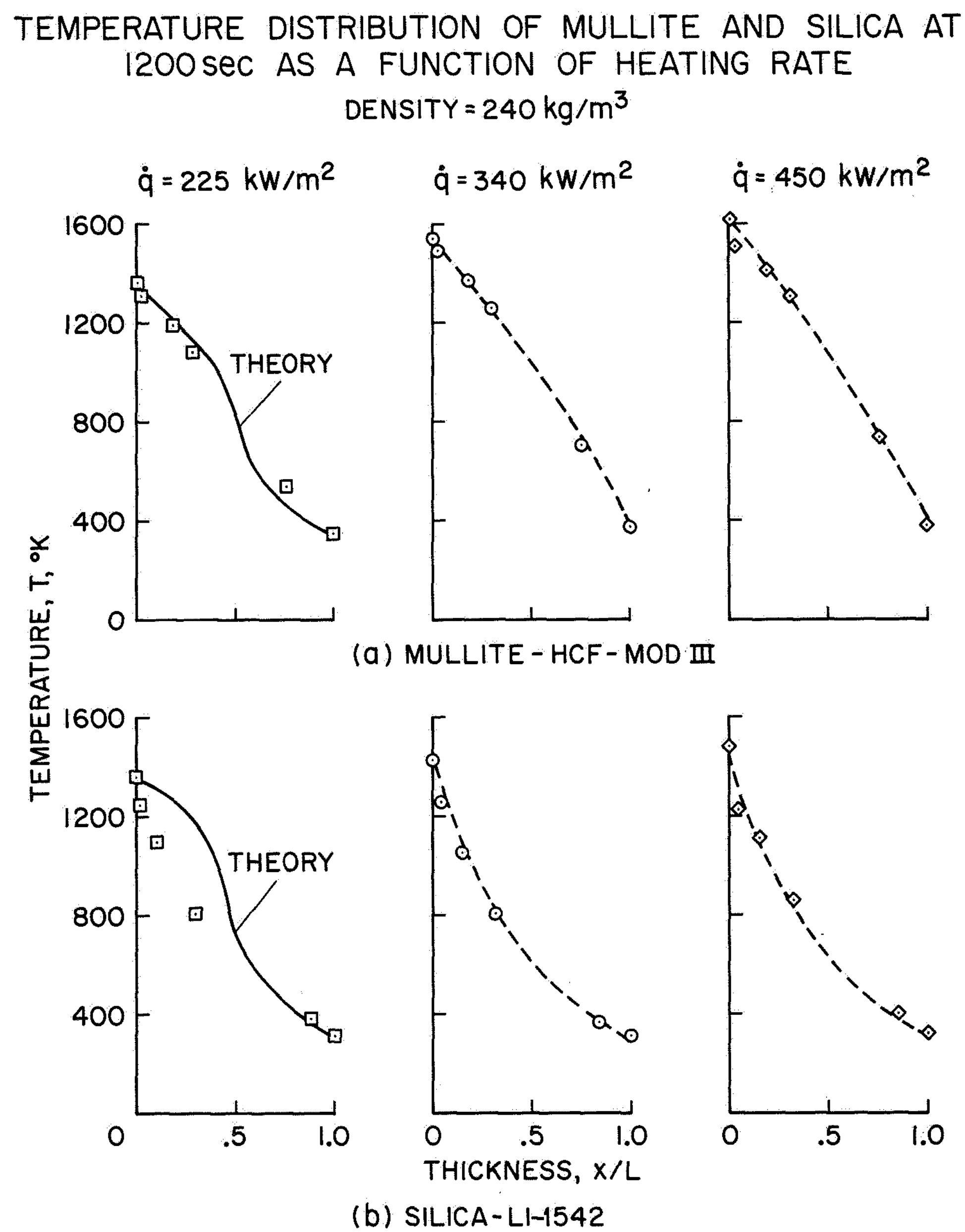
TEMPERATURE DISTRIBUTION OF MULLITE AND SILICA AT 1200 sec AS A FUNCTION OF HEATING RATE
DENSITY = 240 kg/m³
q̇ = 225 kW/m²
q̇ = 340 kW/m²
q̇ = 450 kW/m²
TEMPERATURE, T, °K
1600
1200
800
400
0
THEORY
(a) MULLITE - HCF - MOD III
THEORY
0
.5
1.0
THICKNESS, x/L
(b) SILICA - LI-1542

Figure 10

COMPARISON OF RSI TEMPERATURE DISTRIBUTION AT 1200 SEC ON EQUIVALENT SECTION WEIGHT BASIS (Figure 11)

In this figure the measured internal temperature distributions for the RSI materials in a convective heating environment are compared on an equivalent section weight basis. The temperature distributions through the RSI materials at 1200 seconds into a temperature history simulation using $\dot{q}$ = 225 kw/m^2 (20 Btu/ft^2sec) and $\dot{q}$ = 340 kw/m^2 (30 Btu/ft^2sec) heating rates are plotted as a function of the nondimensional thickness. Starting at the left of the figure, the first comparison was made at $\dot{q}$ = 225 kw/m^2 (20 Btu/ft^2sec) for two 240 kg/m^3 (15 lb/ft^3) density mullite materials (REI-MOD I and HCF-MOD III). A close similarity between the temperature distribution data for the two materials is shown. The second comparison was made at $\dot{q}$ = 340 kw/m^2 (30 Btu/ft^2sec) between two mullite materials made by General Electric (REI-MOD I and REI-MOD 1A) having densities of approximately 240 kg/m^3 (15 lb/ft^3) and 192 kg/m^3 (12 lb/ft^3), respectively. Here the temperature distributions are different. The thermal diffusivity of the REI-MOD I material is greater than the thermal diffusivity of the REI-MOD 1A. The last comparison was also made at $\dot{q}$ = 340 kw/m^2 (30 Btu/ft^2sec) and presents temperature distribution data through a silica (LI-1542) and a mullite (REI-MOD 1A) material having densities of approximately 240 kg/m^3 (15 lb/ft^3) and 192 kg/m^3 (12 lb/ft^3), respectively. The temperature distributions through the two materials indicate that the silica material has a lower thermal diffusivity.

COMPARISON OF RSI TEMPERATURE DISTRIBUTION AT 1200 sec ON EQUIVALENT SECTION WEIGHT BASIS

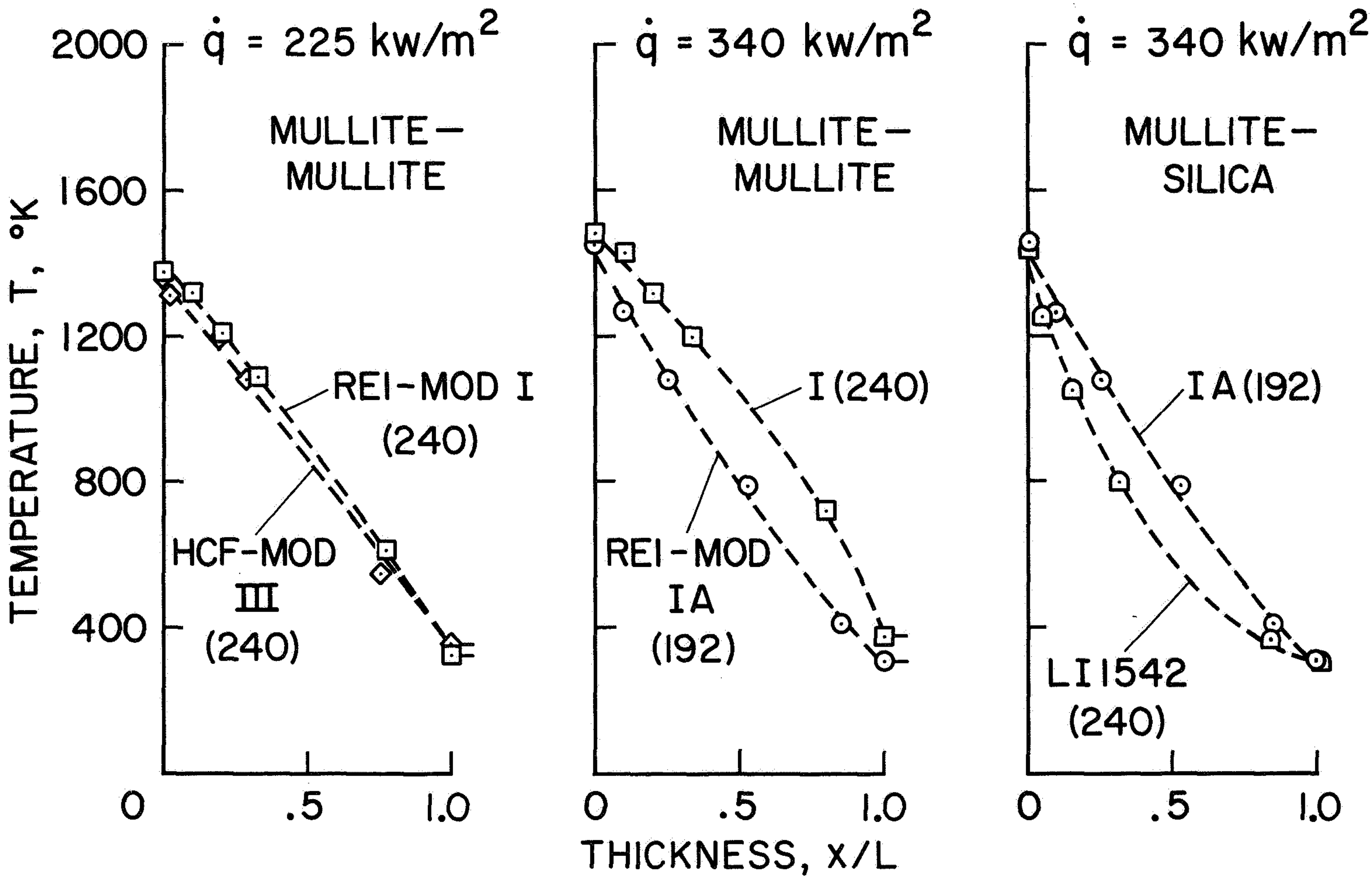

Figure 11

EFFECT OF SURFACE CATALYTIC WALL ACTIVITY ON SURFACE TEMPERATURE OF RSI COATING

(Figure 12)

The surface temperature of a coating at a given convective heating rate depends on both emissivity and its catalytic efficiency in relation to recombination of atomic oxygen and nitrogen species present in the boundary layer. Surface temperature data (utilizing TD-9 and micro optical pyrometers) are plotted as a function of heating rate for the RSI materials. In order to interpret these data, calculated surface temperatures for fully catalytic and fully noncatalytic surfaces (refs 8-9), using pre-test measured total normal emissivity values at T_w = 1367°K (2000°F), are included in the plots. These data show the HCF-MOD III with a $M5_{23}A7P_{700}$ coating was most catalytic and the HCF-MOD I with a M5A7 coating was a little less catalytic. The coatings on the LI-1542, REI-MOD I (SR-2), and REI-MOD 1A (SR-2/XSR-2) were essentially noncatalytic over the range of the heating rates investigated. However, the coating on the LI-1542 sample had a fully catalytic surface at the lowest heating rate $\dot{q}_{HW}$ = 200 kw/m^2 (17.6 Btu/ft^{2}sec). Using bulk and surface chemical analyses it was determined that the LI-1542 coating was impervious and the HCF and REI coatings were permeable to copper and silver vapor contaminants in the arc plasma stream and resulted in copper deposition on the surface of the LI-1542 but not on the others. At heating rates above $\dot{q}_{HW}$ = 200 kw/m^2 (17.6 Btu/ft^{2}sec) the surface temperature on the LI-1542 coating was high enough to prevent the deposition of copper and silver.

In summary, the HCF-MOD III exhibits the largest spread in surface temperature data [1367°K to 1627°K (2000°F to 2470°F)] and the LI-1542 the smallest spread in surface temperature [1367°K to 1467°K (2000°F to 2181°F)] because of the catalytic wall activity. The importance of catalytic wall behavior is realized in the interpretation of arc plasma test results, but has yet to be determined in the design weight of a shuttle heat shield.

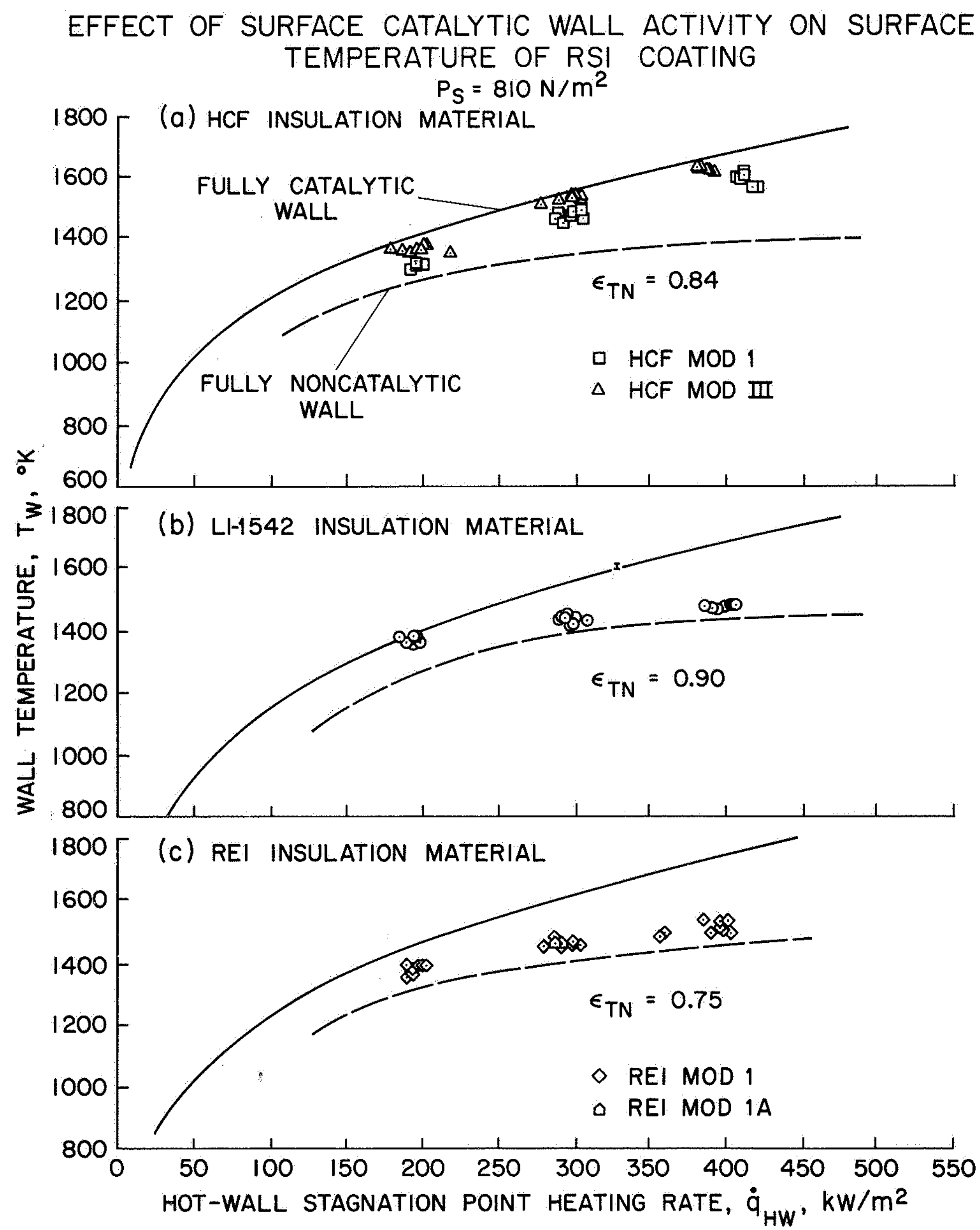
EFFECT OF SURFACE CATALYTIC WALL ACTIVITY ON SURFACE TEMPERATURE OF RSI COATING
PS = 810 N/m2
(a) HCF INSULATION MATERIAL
FULLY CATALYTIC WALL
FULLY NONCATALYTIC WALL
εTN = 0.84
HCF MOD 1
HCF MOD III
(b) LI-1542 INSULATION MATERIAL
εTN = 0.90
(c) REI INSULATION MATERIAL
εTN = 0.75
REI MOD 1
REI MOD 1A
WALL TEMPERATURE, TW, °K
1800
1600
1400
1200
1000
800
600
0
50
100
150
200
250
300
350
400
450
500
550
HOT-WALL STAGNATION POINT HEATING RATE, q̇HW, kW/m2

Figure 12

VARIATION OF OPTICAL PROPERTIES OF RSI COATINGS
AFTER ARC PLASMA TESTING
$\dot{q}$ = 340 kw/m^2

(Figure 13)

The variation of the total hemispherical emittance and the solar absorption coefficient are shown in this figure as a function of arc plasma exposure time at a stagnation point heating rate of $\dot{q}$ = 340 kw/m^2 (30 Btu/ft^{2}sec). Included at the bottom of the figure is the ratio of the two optical properties, $\alpha_s/\varepsilon_{TH}$, an important parameter for thermal control of an orbiting space shuttle. The samples from which the optical properties data were obtained were tested at Ames (square symbols), as well as at Aerotherm (circular symbols) (refs. 2-3). The values of the total hemispherical emittance, and the solar absorption coefficients are calculated from room temperature measurements of spectral hemispherical reflectance and spectral normal reflectance obtained using both a Willey 318 (wavelength range of 2.0 to 15.0 microns) and a Beckman DK1A (wavelength range of 0.3 to 2.3 microns) spectrophotometer. The total 15 micron wavelength limitation of the Willey 318 spectrophotometer (ref. 10). However, calculations of the total hemispherical emittance as a function of temperature show the emittance values at T_w = 1360°K (2000°F) and T_w = 300°K (80°F) are within 10 percent of the data shown (ref. 2). It is, therefore, believed that the total hemispherical emittance and the ratio, $\alpha_s/\varepsilon_{TH}$, are reasonable first approximations for the two above surface temperatures.

The total hemispherical emittance calculated for the HCF-MOD I and HCF-MOD III coatings were in close agreement for arc plasma exposure times greater than 15 minutes. The results for the REI-MOD I and REI-MOD 1A coatings were also similar to each other. Therefore, the data are plotted using only HCF and REI to identify these coatings in the figure. The total hemispherical emittance calculated for the HCF and REI coatings approach constant values of ε_{TH} = 0.79 and ε_{TH} = 0.70, respectively, after roughly 100 minutes of arc plasma exposure time. The emittance value calculated for the LI-1542 coating was relatively unchanged with arc plasma exposure time. Substantial changes in the calculated total hemispherical emittance occurred for both the HCF and REI coatings during early arc plasma exposure times. These changes in emittance have been correlated with surface chemistry changes as discussed by Leiser, et al., in the second part of this study. A 44°K (80°F) increase in the Area 2 surface temperature on the shuttle during peak heating would result from these variations in the total hemispherical emittance of the coatings. The solar absorption coefficients are plotted at the center of the figure. Considerably less change in the solar absorption coefficient occurred for the LI-1542 compared to the HCF and REI coatings. The variation in the solar absorption coefficient appears to depend on the amount of foaming of the low viscosity glass in the RSI coatings. The coefficient decreases with increasing amounts of foaming of the glass as noted from magnified views of the coatings. At the bottom of the figure the ratio $\alpha_s/\varepsilon_{TH}$ is plotted. The results show that the effect of convective heating on this parameter is large for the HCF and REI coatings compared to the LI-1542 coating. In addition, the results show that the variation in total hemispherical emittance during the early arc plasma exposure times has a 10 percent effect on $\alpha_s/\varepsilon_{TH}$ for the HCF coating.

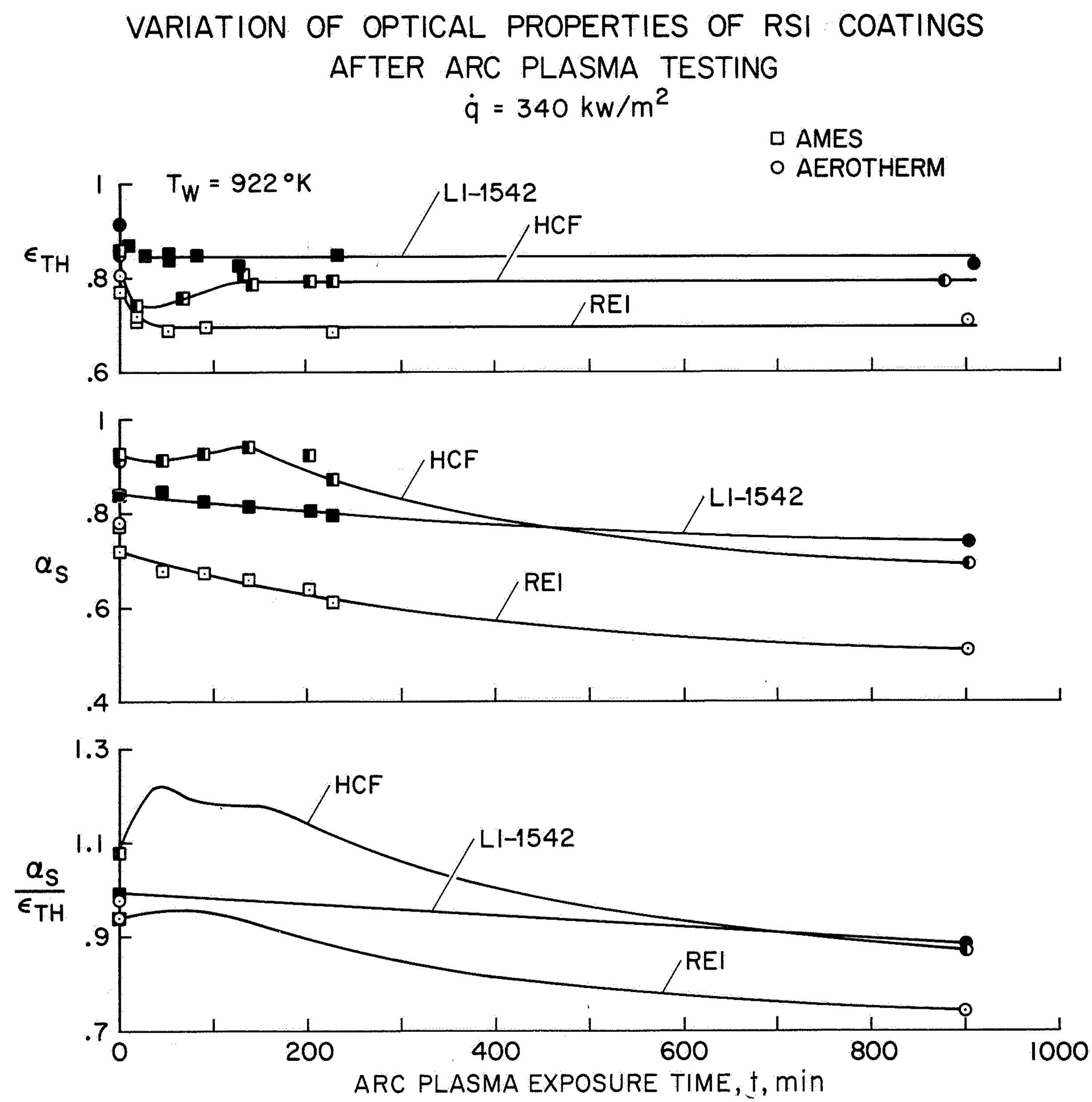
VARIATION OF OPTICAL PROPERTIES OF RSI COATINGS
AFTER ARC PLASMA TESTING
q̇ = 340 kw/m²
AMES
AEROTHERM
T_W = 922 °K
ε_TH
L1-1542
HCF
REI
α_S
α_S / ε_TH
ARC PLASMA EXPOSURE TIME, t, min

Figure 13

CONCLUSIONS

(Figure 14)

This paper has presented results from tests conducted on RSI materials using a preheater in conjunction with an arc plasma stream to simulate shuttle Area 2 and 2P temperature histories. The following observations are noted:

1. Large changes in coating morphology occur on coatings using low viscosity glasses on mullite tiles with glass foaming resulting in decreases in $\alpha_s/\varepsilon_{TH}$ after several entry simulations.

2. The HCF-MOD III coating ($M5_{23}A7P_{700}$), a multiple layer coating, lost its potassium-silicate sealer coating early in the testing and had a nearly fully catalytic surface. The LI-1542 and both REI coatings, basically single layer coatings of pigmented glasses, had nearly fully noncatalytic surfaces.

3. The thermal diffusivity of the 240 kg/m^3 (15 lb/ft^3) density silica material was less than the 192 kg/m^3 (12 lb/ft^3) density mullite material compared on an equivalent section weight basis. In addition, these data show that the thermal diffusivity of the 240 kg/m^3 (15 lb/ft^3) density mullite was greater than that of the 192 kg/m^3 (12 lb/ft^3) density mullite, as would be expected.

4. Large variations in emittance and absorptance were observed on HCF and REI coatings compared to the LI-1542 coating after cyclic arc plasma exposure at a stagnation point heating rate of $\dot{q}$ = 340 kw/m^2 (30 Btu/ft^2sec). The changes in $\alpha_s/\varepsilon_{TH}$ are attributed to both surface chemistry changes and forming of the low viscosity glasses in the coatings caused by the boundary layer convective heating and low surface pressure.

5. From these data it is apparent that the LI-1542 coating was the most stable and the HCF-MOD III the least stable of the coatings based on changes in surface morphology and optical properties.

REFERENCES

1. Goldstein, H.E. and Stewart, D.A.: "Cyclical Arc Jet Tests of Low Density Refractory Surface Insulation Materials." Space Shuttle Materials National Sample Tech. Conference, Society of Aerospace Materials and Process Engineerg, Vol. 3, October 5-7, 1971.

2. Goldstein, H.E., Buckley, J.D., King, H.M. Probst, H.B. and Spiker, I.K.: "Reusable Surface Insulation (RSI) Materials Research and Development." NASA TM X-2570, May 30, 1972.

3. Schaefer, J.W. and Vojvodich, N.S.: "Test Program for Thermal Screening of Candidate Shuttle Vehicle TPS Materials." Final Oral Report, NASA, ARC, Contract NAS2-6445, June 1972.

4. Rinehart, W.A. and Painter, J.H.: "Cyclical Tests of Selected Space Shuttle TPS Materials in a Plasma Arc Tunnel." Technical Monitor Vojvodich, N.S., Contract NAS2-6601, Final Review for NASA, ARC, June 14, 1972.

5. Marvin, J.G. and Sinclair, R.A.: "Convective Heating in Regions of Large Favorable Pressure Gradient." AIAA Journal, Vol. 5, No. 11, November 1967.

6. Stewart, D.A. and Marvin, J.G.: "Convective Heat-Transfer Rates on Large-Angle Conical Bodies at Hypersonic Speeds." NASA TN D-5526, 1969.

7. Centolanzi, F.J., Probst, H.B., Lowell, C.E. and Zimmerman, N.B.: "Arc Jet Tests of Metallic TPS Materials." NASA TM X-62092.

8. Marvin, J.G. and Akin, C.M.: "Pressure and Convective Heat-Transfer Measurements in a Shock Tunnel Using Several Test Gases." NASA TN D-3017, 1965.

9. Pope, R.B.: "Stagnation-point Convective Heat Transfer in Frozen Boundary Layers." AIAA Journal, Vol. 6, No. 4, 1968, pp 619-626.

10. Holman, J.P.: "Heat Transfer," McGraw-Hill Book Company, New York, Chapter 8, 1968, pp 211-264.